Journal of Visualized Experiments

Laser micro-irradiation to study DNA recruitment during S phase

--Manuscript Draft--

Article Type:	Invited Methods Collection - JoVE Produced Video
Manuscript Number:	JoVE62466R1
Full Title:	Laser micro-irradiation to study DNA recruitment during S phase
Corresponding Author:	Gergely Rona UNITED STATES
Corresponding Author's Institution:	
Corresponding Author E-Mail:	gergely.rona@nyulangone.org
Order of Authors:	Bearach Miwatani-Minter
	Gergely Rona
Additional Information:	
Question	**Response**
Please indicate whether this article will be Standard Access or Open Access.	Open Access (US$4,200)
Please specify the section of the submitted manuscript.	Biology
Please indicate the **city, state/province, and country** where this article will be **filmed**. Please do not use abbreviations.	New York, New York, USA
Please confirm that you have read and agree to the terms and conditions of the author license agreement that applies below:	I agree to the Author License Agreement
Please provide any comments to the journal here.	Revised version of our manuscript (tracking number # JoVE62466)
Please indicate whether this article will be Standard Access or Open Access.	Open Access ($3900)

TITLE

Laser Micro-Irradiation to Study DNA Recruitment During S phase

AUTHORS AND AFFILIATIONS:

Bearach Miwatani-Minter[1,2], Gergely Rona[1,2,3]

[1]Department of Biochemistry and Molecular Pharmacology, New York University School of Medicine, New York, USA.

[2]Laura and Isaac Perlmutter Cancer Center, New York University School of Medicine, New York, USA.

[3] Howard Hughes Medical Institute, New York University School of Medicine, New York, USA.

Corresponding Author:

Gergely Rona (Gergely.Rona@nyulangone.org)

Email Address of Co-Author**:**

Bearach Miwatani-Minter (Bearach.Miwatani-minter@nyulangone.org)

KEYWORDS:

micro-irradiation, S phase, PCNA foci, DNA damage, protein recruitment, EXO1b, 405 nm laser

SUMMARY:

This protocol describes a non-invasive method to efficiently identify S-phase cells for downstream microscopy studies, such as measuring DNA repair protein recruitment by laser micro-irradiation.

ABSTRACT

DNA damage repair maintains the genetic integrity of cells in a highly reactive environment. Cells may accumulate various types of DNA damage due to both endogenous and exogenous sources such as metabolic activities or UV radiation. Without DNA repair, the cell's genetic code becomes compromised, undermining the structures and functions of proteins and potentially causing disease.

Understanding the spatiotemporal dynamics of the different DNA repair pathways in various cell cycle phases is crucial in the field of DNA damage repair. Current fluorescent microscopy techniques provide great tools to measure the recruitment kinetics of different repair proteins after DNA damage induction. DNA synthesis during the S phase of the cell cycle is a peculiar point in cell fate regarding DNA repair. It provides a unique window to screen the entire genome for mistakes. At the same time, DNA synthesis errors also pose a threat to DNA integrity that is not encountered in non-dividing cells. Therefore, DNA repair processes differ significantly in S phase as compared to other phases of the cell cycle, and those differences are poorly understood.

The following protocol describes the preparation of cell lines and the measurement of dynamics of DNA repair proteins in S phase at locally induced DNA damage sites, using a laser-scanning

confocal microscope equipped with a 405 nm laser line. Tagged PCNA (with mPlum) is used as a cell cycle marker combined with an AcGFP-labeled repair protein of interest (i.e., EXO1b) to measure the DNA damage recruitment in S phase.

INTRODUCTION

Several DNA repair pathways have evolved to address the different types of DNA lesions that can arise in cells, all of which are highly regulated in both space and time. One of the most vulnerable periods of the cell cycle is S phase, when DNA synthesis occurs. While proliferation is fundamental to life, it also provides a major challenge. Cells need to ensure faithful replication of their genome to avoid mutations to be passed down to future generations. Consequently, proliferation provides a therapeutic point of intervention that has been employed for the development of therapeutic approaches in the field of oncology.

All the major techniques used for studying protein recruitment at DNA lesions have their strength and limitation. Micro-irradiation has better spatial and temporal resolution[1] than most of the alternative methods like immunofluorescent imaging of ionizing radiation-induced foci (IRIF), chromatin-immunoprecipitation (ChIP), or biochemical fractionation. However, micro-irradiation lacs the robustness of the aforementioned techniques that can sample a large number of cells at the same time.

To investigate DNA repair in S phase, one must be able to distinguish S phase cells in an asynchronous cell culture population. There are many well-known methods to address this, involving either the synchronization of cells, or visualization of the different cell cycle phases. However, both approaches introduce significant challenges and possible artefacts. Chemical synchronization methods widely used to enrich cells in early S phase (e.g., double thymidine block, aphidicolin, and hydroxyurea treatment) achieve synchronization through the induction of replication stress and eventually DNA damage itself. This limits the use of these methods to study DNA repair processes in S phase[2]. Synchronization through serum starvation and release is only applicable to a limited number of cell lines, largely excluding cancer cell lines which rely less on growth factors for cell-cycle progression compared to non-transformed cell lines. The Fluorescence Ubiquitin Cell Cycle Indicator (FUCCI) system is a particularly useful tool to study the cell cycle, but it has a fundamental limitation when differentiating between S and G2 cell-cycle phases[3].

Here it is shown that using fluorescently tagged PCNA as a non-invasive marker for S phase limits the drawbacks of chemical cell-cycle synchronization methods, while allowing for more specificity and flexibility than the FUCCI system. As a single marker, not only can PCNA highlight S-phase cells in an asynchronous population, but it can also show the exact progression of cells within S phase (i.e., early, mid, or late S-phase)[4]. Low expression levels of exogenous, tagged PCNA ensures minimal interference with both cell cycle progression and DNA repair processes. Importantly, PCNA also serves as an internal control for proper DNA damage induction as it is involved in the repair of several DNA lesions and is recruited to locally induced DNA damage sites[1,4].

The experiments presented here demonstrate how to measure the recruitment dynamics of EXO1b in S phase and how this is affected by the well-established PARP inhibitor, olaparib. EXO1b nuclease activity is relevant to a wide range of DNA repair pathways including mismatch repair (MMR), nucleotide excision repair (NER), and double-stranded break (DSB) repair. In S phase, EXO1b plays a major role in homologous recombination (HR) through the formation of 3' ssDNA overhangs during DNA resection[5]. EXO1b has been further implicated in DNA replication with roles in checkpoint activation to restart stalled DNA forks as well as primer removal and Okazaki fragment maturation at the lagging strand during strand displacement in replication[5]. EXO1b recruitment to damaged DNA sites is regulated by the direct interaction with poly (ADP-ribose) (PAR)[6,7]. Due to the numerous cell-cycle specific implications of EXO1b, it is an excellent choice for S-phase specific recruitment studies using PCNA.

PROTOCOL

1. Cultivation of human osteosarcoma-derived cells (U-2 OS)

NOTE: U-2 OS cells are ideal for these studies as they have a flat morphology, large nucleus and strongly attach to several surfaces, including glass. Other cell lines with similar characteristics could also be used.

1.1. For cultivation of U-2 OS cell lines, use McCoy's 5A medium supplemented with 10% fetal bovine serum (FBS) and antibiotics (100 U/mL penicillin and 100 µg/mL streptomycin). Incubate cells at 37 °C in a humidified atmosphere containing 5% CO_2. For microscopy studies, maintain cell culture in a 10 cm dish to provide sufficient cell count.

1.2. When cells approach 90% confluency (~7 x 10^6 cells/10 cm dish), split the cells.

1.2.1. Rinse cells with PBS to wash away trypsin inhibitors contained within the serum.

1.2.2. Add 1 mL of Trypsin-EDTA and ensure that the cell layer is equally covered.

1.2.3. Incubate at 37 °C until the cell layer is lifted off the plate (approximately 6 min).

1.2.4. Resuspend the trypsinized cells in serum containing media to inactivate the trypsin and add 1/10^{th} of the volume (~0.7 x 10^6 cells) into a new 10 cm plate containing 10 mL of supplemented growth medium.

1.3. Prior to experimentation, routinely test cells for mycoplasma contamination using the Universal Mycoplasma Detection kit following the manufacturer's recommendation.

2. Retroviral infection

NOTE: For BSL-2 safety measures and while working with recombinant viruses, please refer to: NIH Guidelines, Section III-D-3: Recombinant viruses in tissue culture.

2.1. Seed 4 x 10^6 HEK293T cells to achieve ~60% confluency within 24 h after plating into a 10 cm culture dish.

2.1.1. For cultivating HEK293T please follow the cultivation steps of U-2 OS described in 1.1-1.3 of this protocol. For HEK293T substitute McCoy's 5A medium for DMEM. Be sure to always gently wash HEK293T cells as they attach to tissue culture plates weakly.

2.2. Transfect HEK293T cells using lipid-based transfection reagent for viral packaging of plasmids.

2.2.1. For retroviral vectors, combine 1.5 µg of VSV-G (Addgene #8454) and 1.5 µg of pUMVC (Addgene #8449) packaging vectors along with 3 µg of the vector containing the gene of interest (in a retroviral vector backbone with puromycin resistance) into 250 µL of Opti-MEM reduced serum media in a microcentrifuge tube. Add 1 µL of P3000 reagent for each µg of DNA added into the Opti-MEM/DNA mixture (in this case 6 µL) and mix gently by tapping. Do not vortex or pipette up and down.

2.2.2. In another microcentrifuge tube, combine 2 µL per µg DNA (in this case 12 µL) of transfection reagent with 250 µL of Opti-MEM reduced serum media.

2.2.3. Combine the two mixtures (500 µL combined, do not vortex, only mix by gentle tapping) and let it incubate for 15 min at room temperature.

2.2.4. Carefully, add the mixture dropwise to the seeded HEK293T cells without detaching the cells. Swirl the plates gently.

2.3. Viral infection to generate stable cell lines.

2.3.1. Remove the virus containing supernatant from the HEK293T cells 72 h after transfection. Carefully filter the solution with a 0.45 µm filter to remove cell debris and detached cells. Optionally, add 8 µg/mL polybrene to the viral supernatant to facilitate viral infection.

2.3.2. Add virus containing supernatant to U-2 OS cells at ~50% confluency in a 10 cm dish (~3 x 10^6 cells). Seed the U-2 OS cells the day before.

2.3.3. Infect for 6-16 h before removing and discarding the virus-containing supernatant.

NOTE: To achieve the desired amount of overexpression for the gene of interest, incubate a series of viral dilutions for a fixed amount of time. Check the expression levels of the transgene in each newly established cell line with western blot comparing it to endogenous levels.

2.3.4. Allow cells to select in the presence of appropriate antibiotics (for 3-4 days in case of puromycin at 2 µg/mL final concentration) and verify the expression of the fluorescent protein

tagged gene of interest under a microscope.

2.3.5. Repeat these steps to generate double labeled cell lines. In the experiments presented here mPlum-PCNA was expressed from a retroviral vector (pBABE) combined with EXO1B-AcGFP, also expressed from a retroviral vector (pRetroQ-AcGFP1-N1).

3. Preparation of cells for micro-irradiation

3.1. Plating cells: 24 h before the experiment, plate a total of 8.0 x 10^4 cells into a volume between 500 µL-1 mL of media (for roughly 70% confluency) on a four well chambered coverglass with a No. 1.5 borosilicate glass bottom which delivers ideal results for high-magnification confocal microscopy and laser micro-irradiation. A higher cell confluency allows for more cells measured in a single field of view (FOV); however fully confluent slides will introduce cell cycle irregularities.

3.2. Imaging media: An hour before micro-irradiation, exchange regular growth medium for FluoroBrite DMEM supplemented with 10% FBS, 100 U/mL penicillin and 100 µg/mL streptomycin, 15 mM HEPES (pH=7.4) and 1 mM sodium-pyruvate. This imaging media helps maximize the signal-to-noise ratio allowing the detection of very dim fluorescence. Since it contains HEPES, it also stabilizes pH in the absence of a 5% CO_2 atmosphere.

3.3. Apply any additional treatment before the imaging at this step. In the experiments presented here, cells were pre-treated one hour before imaging with either olaparib (PARP inhibitor, at 1 µM final concentration) or a vehicle control (DMSO)[1,8,9].

4. Preparing the microscope and selecting S phase cells for imaging.

4.1. Use a confocal system that has the similar properties as the system outlined here for best results. The experiments presented here were performed using a confocal microscope mounted on an inverted microscope stand (see **Table of Materials**).

NOTE: The microscope used here was equipped with a 50 mW 405 nm FRAP laser module, and a 60x 1.4 NA oil plan-apochromat objective. The confocal scanhead had two scanner options: a galvano scanner (for high resolution) and resonant scanner (for high-speed imaging).

4.1.1. Introduce fluorescence recovery after photobleaching (FRAP) laser to the sample via a software controlled XY galvano device. Use a 488 nm laser line to excite AcGFP and a 561 nm or 594 nm laser line to excite mPlum.

NOTE: The following filter combination gives optimal results: using a 560 nm long pass filter, emission light with a wavelength lower than 560 nm was passed through a 525/50 nm emission filter for AcGFP, while emission light with a wavelength higher than 560 nm was passed through a 595/50 nm emission filter for mPlum. Any appropriate filter set (e.g., FITC/TRITC, GFP/mCherry, FITC/TxRed) that ensures minimal fluorescence bleed-through could be used.

4.2. Turn on the environmental chamber and the microscope components.

4.2.1. Turn on the heating (stage, objective, and environmental chamber when possible), CO_2 supply and the humidity regulator at least 4 h before the start of the experiment to ensure thermal equilibration for stable image acquisition.

4.2.2. Initialize light sources along with the laser lines at least 1 h before the transfer of the cells to the microscope.

4.3. Select S-phase cells in an asynchronous population using fluorescently tagged PCNA as a marker. Do this by following the steps below.

4.3.1. Look for the unique localization pattern of the mPlum-tagged PCNA in S phase making identification of this cell cycle phase possible. PCNA has a completely homogeneous distribution in the nucleus in G1 and G2 phases of the cell cycle, while being excluded from the nucleoli. In S-phase, PCNA forms foci at the location of replisomes in the nucleus. **Figure 1** shows the different patterns of PCNA foci throughout S-phase, which makes it possible to even differentiate early, mid, and late S-phase.

4.3.2. Look through the ocular to select an FOV that has enough S-phase cells for micro-irradiation. Asynchronous U-2 OS cells usually have 30-40% of their population in S phase.

4.3.3. Try to avoid extremes in expression levels (bright and dim cells alike) for both PCNA and the protein of interest (POI), in this case EXO1b-AcGFP, which could lead to experimental artefacts.

4.3.4. When finding a suitable FOV, try to avoid scanning the field for a long time to minimize photobleaching and unwanted DNA damage.

4.3.5. Set the desired region of interest (ROI) for micro-irradiation. Using the associated software (see **Table of Materials**), set desired ROI by first inserting binary lines (set the desired number of lines and spacing). Click **Binary,** then click **Insert line | Circle | Ellipse** to draw the desired number of lines.

4.3.6. Convert these binary lines to ROIs and finally convert these ROIs into stimulation ROIs. To do that, first click **ROI,** then click **Move Binary to ROI**, then right click on any of the ROIs and select **Use as Stimulation ROI: S1**. Place these lines in the FOV to pass through the nucleus of the cells. ROIs with a length of 1024 pixels that spanned the entire FOV were used throughout the protocol.

5. Micro-irradiation for immunofluorescence staining or time lapse imaging.

5.1. Determining optimal micro-irradiation settings.

5.1.1. Before micro-irradiation of the cells, take a higher resolution image of the FOV to identify PCNA foci for later analysis. Instead of sequential scanning, simultaneously record both optical channels used (green and red), to avoid cell movement between scanning at the two wavelengths. For proper resolution of the foci use at least 1024 x 1024 pixels/field resolution with 1x zoom (0.29 µm pixels size on the imaging system used here), with 1/8 frame/s scanning speed (4.85 µs/pixel) with 2x averaging. Once these parameters are set in the **A1 LFOV Compact GUI** and the **A1 LFOV Scan Area** windows, hit the **Capture** button to record the FOV.

NOTE: It is important to maintain the same pixel size throughout experiments to ensure comparable results.

5.1.2. To set up the micro-irradiation, open the **ND Stimulation** tab in the imaging software to access the **Time schedule (A1 LFOV / Galvano Device)** window. This uses the galvano scanners to acquire a series of pre-stimulation images, stimulate (using the LUN-F 50 mW 405 nm FRAP laser), and then acquire a series of post-stimulation images again using the galvano scanners. First set up three phases in the **Time schedule** window. In the **Acq/Stim** column select **Acquisition | Bleaching | Acquisition** for the three phases respectively. For the bleaching phase, set **S1** as the ROI.

NOTE: In the experiment presented here, no images are acquired during the stimulation phase.

5.1.3. In the **Galvano XY window**, set up the key factors for micro-irradiation: 405 nm laser power output, dwell time (iteration is 1 by default on this system). In the experiments presented here, cells were irradiated with the 405 nm FRAP laser (50 mW at the fiber tip) at 100% power output with a 1000-3000 µs dwell time.

NOTE: Because laser dwell time is on a per pixel basis, as long as pixel size remains the same, the relationship between the dwell time and power density will be comparable between different FOVs. **Figure 2A** shows the use of DNA damage response (DDR) pathway specific proteins (FBXL10 for DSBs and NTHL1 for oxidative base damage) to optimize laser power settings for specific damage induction. These stable cell lines were generated with viral infection following section 2 of the protocol.

5.2. Time lapse imaging.

5.2.1. Set up time lapse imaging for the desired time window and intervals using the **Time schedule**, **A1 LFOV Compact GUI** and the **A1 LFOV Scan Area** windows. In the experiments presented here, the recruitment of EXO1b and PCNA was imaged for 12 min, scanning the FOV every 5 seconds, at 1024 x 1024 pixels/field, using 1x zoom (resulting in 0.29 µm pixels size on the imaging system used here) with 0.35 frame/s scanning speed (1.45 µs/pixel) without averaging to reduce photo-bleaching.

5.2.2. Optimize the **laser power %**, **gain** and **offset settings** to reduce photo-bleaching during

the imaging in the **A1 LFOV Compact GUI** window. If one aims to measure both POI and PCNA, use simultaneous scanning instead of sequential scanning, to avoid cell movement between scanning the field for the two separate fluorophores.

5.2.2.1. The imaging system was used with the following settings. For the 488 nm laser line (20 mW): 7% laser power, gain: 45 (GaAsP detector) with and offset of 2, for the 561 nm laser line (20 mW): 4% laser power, gain 40 (GaAsP detector) with and offset of 2.

5.2.3. Depending on the kinetics of the protein, extend or shorten the interval between images or the duration of the total time lapse. In the **Time Schedule** window, set the desired **Interval** and **Duration** for the third phase Acquisition row.

5.2.4. Press **Run now** to execute the micro-irradiation and the subsequent time lapse imaging.

5.2.5. At the end of the time lapse imaging, save the stimulation ROIs as separate images, which will be a useful aid to identify the coordinates of micro-irradiation in any downstream software used for analysis.

5.3. Immunofluorescence staining.

NOTE: Step 5.1.3 and **Figure 2A** demonstrates the use of known DNA repair proteins to assess the types of DNA lesions introduced by micro-irradiation. Certain DNA lesions can also be detected by using specific antibodies after fixing the cells. It is also possible to detect the recruitment of the POI by antibody detection of the endogenous protein. The visualization of γH2A.X to check for DSBs is demonstrated below (**Figure 2B**). **Figure 3** shows the consistency of PCNA localization and recruitment throughout cell cycle for both endogenous and exogenous tagged PCNA.

5.3.1. After step 5.1.3, take just one image after micro-irradiation to ensure proper FRAP event based on the recruitment of mPlum-PCNA. Take note of the exact coordinates of the FOV to to find the field later after the immunofluorescent labeling.

5.3.2. Take the cell culture chamber out of the microscope and incubate cells at 37 °C in a humidified atmosphere containing 5% CO_2 for 5-10 min.

NOTE: Paraformaldehyde (PFA) is toxic, and work should be done in a well-ventilated area or a fume hood. All subsequent washing and incubation will be done with 0.5 mL volumes in the 4 well chamber slide. After the incubation time, wash the cells with 0.5 mL of PBS (137 mM NaCl, 2.7 mM KCl, 8 mM Na_2HPO_4, and 2 mM KH_2PO_4) and fix with 0.5 mL of 4% PFA in PBS for 10 min at room temperature (RT).

5.3.3. Wash the cells once with PBS, then wash them with 50 mM NH_4Cl to quench residual PFA.

5.3.4. Permeabilize the cells for 15 min at RT with 0.1% Triton X-100 in PBS.

5.3.5. Block the samples for 1 h with blocking buffer (5% FBS, 3% BSA, 0.05% Triton X-100 in PBS).

5.3.6. Remove the blocking solution and add the diluted primary antibody (anti-γH2A.X, 1:2000) in blocking buffer for 1 h at RT.

5.3.7. Wash the wells with blocking buffer 3 x 10 min.

5.3.8. Add diluted secondary antibody (anti-mouse Alexa 488 Plus conjugate, 1:2000) in blocking buffer for 1 h at RT.

5.3.9. Wash the wells with blocking buffer 3 x 10 min.

5.3.10. Counterstain the nucleus with 1 µg/mL DAPI solution in PBS for 15 min.

5.3.11. Wash the cells once with PBS. The imaging can be performed directly in PBS or a PBS solution with antifade reagents (e.g., AFR3) to reduce photobleaching.

6. Recruitment analysis

NOTE: **Figure 4A** shows representative images of Exo1b and PCNA recruitment in the presence of DMSO or olaparib. **Figure 4B** shows a representative image for data analysis. Mean fluorescence values were calculated by measuring mean AcGFP intensities using a rectangle along the laser track highlighted by the mPlum-PCNA (A, yellow rectangles) across different timepoints using ImageJ. PCNA can serve as an internal control to highlight successful irradiation along the ROI coordinates. Similarly, mean AcGFP fluorescence values were also calculated for undamaged regions of the nucleus (B, blue rectangles). Background signal intensity was measured in unpopulated areas (C, red rectangles) and was subtracted from the mean fluorescent values (Figure A and B). Thus, the relative mean fluorescent unit (RFU) for each data collection point was calculated by the equation RFU = (A − C)/ (B − C)[8,9]. The resulting RFU values of the micro-irradiated region is normalized to the RFU values prior to micro-irradiation.

6.1. For defining the region A of the micro-irradiated site, exclude nucleolar regions, replication foci, and irregular nuclear regions of the cell from measurement. Hold **shift** key in between drawing two ROIs in Fiji to group two separate regions as one.

NOTE: Protein recruitment will vary among different genes and irradiation conditions; thus, the size of region A must be determined individually. Once pixel width of region A is determined, it should remain constant for any comparative recruitments. In the experiments presented here, 7 pixel width rectangles were used.

6.2. Exclude cells, that moved during the duration of the recorded videos, from analysis. To include highly mobile cells, the described analysis must be carried out frame-by-frame.

6.3. To visualize the recruitment profile, plot the normalized RFU values against time using a statistical software.

6.4. Calculate the difference at an indicated time-point between DMSO and olaparib (n=31) treatment using a Mann-Whitney test.

REPRESENTATIVE RESULTS

Cells address each type of DNA lesion in a specific manner that also depends on which cell cycle phase they are in. For example, following micro-irradiation, double-stranded breaks (DSB) will be processed either by non-homologous end joining (NHEJ) or HR depending on the cell cycle phase. Nucleases acting most extensively during the S and G2 phases of the cell cycle create DNA overhangs that are crucial for proper HR. To promote the evaluation of cells in S phase, PCNA was employed as a single-color cell cycle marker. **Figure 1A** shows the localization profile of mPlum-PCNA during cell cycle progression. PCNA has a completely homogeneous distribution in the nucleus in G1 and G2 phase (while also being mostly excluded from the nucleoli). In S phase, PCNA localizes to sites of DNA replication, which can be visualized as bright spots in the nucleus. In early S phase cells, the spots are relatively small and equally distributed throughout the nucleus of the cell. Progressing into mid S phase, the spots become blurred and localize more towards the perimeter of the nucleus and the nucleoli. In late S phase, the spots reduce in numbers but become increasingly large as PCNA concentrates at late replication sites (**Figure 1B**). Importantly, exogenous PCNA expression from the pBABE vector backbone was less than the endogenous levels but was enough for detection by microscopy which minimizes potential artefacts in cell cycle progression and DDR. **Figure 1C** shows the extent of PCNA overexpression compared to endogenous levels. Please note that the band corresponding to mPlum-PCNA migrates slower due to its larger size.

We aimed to introduce DSBs during micro-irradiation to investigate the PARP1/2-dependent recruitment of EXO1b to these lesions in S phase. **Figure 2A** shows that low doses of energy (1000 µs dwell time) do not induce the recruitment of EGFP-FBXL10, a DSB responder (component of the FRUCC complex [8]), while it was sufficient to induce the recruitment of NTHL1-mCherry, a base excision repair (BER) pathway protein, recruiting to sites of oxidative DNA damage[10-12]. At 3000 µs dwell time, both EGFP-FBXL10 and NTHL1-mCherry recruit, demonstrating a laser output that generates both oxidative lesions and DSBs. Strengthening these results, **Figure 2B** shows immunofluorescence staining against γH2A.X (DSB marker), which is clearly more apparent when using higher energy doses. PCNA serves as both a cell cycle marker and a marker for successful micro-irradiation, as it adequately recruits with both laser dwell time settings. Importantly, both exogenous and/or endogenous fluorescent protein-tagged PCNA can be used for this reporter function as they behave similarly (**Figure 3**). Endogenously tagged PCNA was engineered by inserting mRuby in frame with the first exon into one allele of the PCNA locus[13] (the cell line was a kind gift of Jörg Mansfeld).

Figure 4A and **Figure 4C** shows the recruitment of AcGFP-tagged EXO1b in S phase cells. EXO1b reaches maximum level of accumulation at micro-irradiation sites around 1 minute and then

slowly starts disengaging from the DNA lesions afterwards. Enrichments at micro-irradiation sites are denoted by a > 1 relative fluorescence unit on the graph. In the presence of olaparib, accumulation of EXO1b at the laser stripe at 1 minute is significantly less compared to the vehicle control. These results are in agreement with the literature[6,7]. **Figure 4B** demonstrates representative regions for quantification (areas A, B, and C) as described in point 6 in the protocol. **Figure 4D** shows the comparable expression levels of endogenous EXO1b and exogenous EXO1b-AcGFP in cells used for micro-irradiation.

FIGURE LEGENDS

Figure 1: Localization pattern of PCNA. (**A**) Images show localization pattern of stably integrated, exogenous PCNA throughout the cell cycle in U-2 OS cells. (**B**) Images show PCNA foci patterns in different stages of S phase (early, mid, and late) in U-2 OS cells. (**C**) Western blot showing endogenous and exogenous levels of PCNA in the U-2 OS cells used for imaging. Scale bar represents 20 µm.

Figure 2: Induction of DSBs through optimized laser power output. (**A**) Laser settings can be optimized to induce different forms of DNA damage. U-2 OS cells stably expressing both EGFP-FBXL10 and NTHL1-mCherry were used to identify DSBs and sites of oxidative lesions, respectively. Micro-irradiation with a 405 nm laser line was carried out on asynchronous U-2 OS cells with either 1000 µs or 3000 µs dwell time. Scale bar represents 20 µm. (**B**) Immunofluorescent staining against γH2A.X was done on human retinal pigment epithelial cells (hTERT RPE-1) having mRuby-tagged endogenous PCNA. Cells were fixed and processed 5 minutes after micro-irradiation with either 1000 µs or 3000 µs dwell time. Scale bar represents 20 µm.

Figure 3: Comparable recruitment of endogenous mRuby-PCNA and exogenous mPlum-PCNA to micro-irradiation sites at 1000 µs or 3000 µs laser dwell time. Both endogenous and exogenous tagged PCNA form replication foci during S phase.

Figure 4: PARP1/2-dependent recruitment of EXO1b in S phase. U-2 OS cells stably expressing EXO1b-AcGFP and mPlum-PCNA were micro-irradiated with 405 nm FRAP laser line using 3000 µs dwell time. (**A**) Representative images of micro-irradiated cells at the indicated time points after pre-treatment with either vehicle control (DMSO) or olaparib (1 µM). Scale bar represents 20 µm. (**B**) Representative images of defined regions of A, B, and C areas for the recruitment analysis. Scale bar represents 20 µm. (**C**) DNA damage recruitment dynamics was captured by live cell imaging. Relative mean fluorescence values and images were acquired every 5 s for 12 min. For each condition, ≥30 cells were evaluated. Mean relative fluorescence values (solid black lines) and standard error (range visualized by a shaded area) were plotted against time. Dashed line shows recruitment values at 1 min after micro-irradiation. The difference between DMSO (n=32) and olaparib (n=31) treatment was calculated using a Mann-Whitney test. Asterix denotes $p<0.0001$. (**D**) Western blot compares the expression levels of endogenous EXO1b and exogenous EXO1b-AcGFP in cells used for micro-irradiation.

DISCUSSION:

Critical steps and potential protocol troubleshooting/modifications

Proper tissue culture vessel for micro-irradiation is critical for success. Most high-resolution imaging systems are optimized for 0.17 mm cover glass thickness. Using higher or lower thickness imaging chambers or ones made from plastic polymers (not optimized for 405 nm imaging), can significantly reduce image quality. When using glass surfaces, make sure that they are tissue-culture treated to enhance cell adhesion. If they are not tissue-culture treated, these chambers will need to be coated, for example, with poly-D-lysine before seeding the cells. When plating cells into the chambered coverglass, ideal cell density is paramount to avoid cell cycle irregularities and additional stress to the cells. Proper thermal equilibration of the microscope components prior to experimentation to maintain a stable temperature is crucial for both maintaining the focus throughout the time lapse imaging and is also necessary to ensure a homogeneous DDR across time and samples.

It is critical that cells are in a healthy condition prior to micro-irradiation to reduce artefactual data. If cells have irregular morphology post-infection/selection, allow cells to progress through multiple passages until morphology returns to normal. Always make sure that the cells lines used are free of mycoplasma contamination. Among the many adverse effects of mycoplasma infection, it also causes DNA damage to the host cells and could affect their DDR pathways[14,15]. The most sensitive way to detect mycoplasma in the cell culture is through PCR (versus. detection with DAPI or Hoechst).

Optimal overexpression of the repair protein of interest should be comparable to endogenous levels, however, high enough for detection. The promoter used on the viral vectors, the viral titer during infection, and the length of the infection time can all be adjusted for ideal expression levels. For consistent results, isolate individual cell clones to ensure homogeneous expression levels and normal cell morphology. It is recommended to use vector constructs that do not overexpress tagged PCNA at higher than endogenous levels for proper cell-cycle and DNA repair marker function. Even low levels of PCNA overexpression are sufficient to discriminate S-phase cells. Retroviral pBABE vectors have been successfully used for this purpose (Addgene #1764, #1765, #1766, #1767). PCNA can be tagged with any monomeric red (*e.g.,* mPlum, mCherry, mRuby, etc.) or monomeric green fluorescent proteins (e.g., mEGFP, AcGFP, mWasabi, mNeonGreen, mEmerald, etc.) which could then be combined with an alternately tagged POI. Overexpressing a fluorescently tagged POI has some limitations and considerations. Fluorescent tags may disrupt normal protein function and localization. Thus, the location of the tag (N or C-terminal) must be considered. Always use monomeric fluorescent proteins, as oligomerization of non-monomeric variants can affect the function of the POI.

The laser settings must be determined for each imaging system as many components of the optical path will affect the actual power delivered into the cells. Laser micro-irradiation can cause several types of DNA lesions depending on the excitation wavelength, the power output of the FRAP laser and if any pre-sensitizing agents (like Bromodeoxyuridine or Hoechst) were used. 405 nm lasers can cause oxidative DNA damage, single and double stranded breaks[16,17]. By using higher laser output settings, the amount of DSBs increases. In this protocol pre-sensitization

methods were not utilized, but these techniques are greatly covered in the literature and re-capped in the discussion below. In our opinion, the best way to test if the desired lesion is generated is by testing for the recruitment of known DNA damage pathway specific genes. Recruitment of NTHL1 or OGG1, components of the BER pathway, suggests the induction of oxidized DNA bases[10,11,17-19], while FBXL10 or XRCC5 indicate the presence of DSBs[8,20,21]. Recruitment of XRCC1 can indicate both the presence of oxidized DNA bases and single stranded breaks (SSB)[22,23]. XPC (i.e., RAD4) is a good indicator of NER that removes the bulky DNA adducts generated by ultraviolet light (UV)[17,24]. Because recruiting exogenous proteins may introduce certain irregularities, immunofluorescent staining of endogenous DNA repair proteins or markers (like γH2A.X for double stranded breaks) can confirm the presence of specific DNA lesions. Alternatively, antibodies raised against specific types of DNA lesions could also be used. To adjust the delivered laser power, both the dwell time and the laser power can be changed.

With the help of mathematical modeling, a detailed kinetic analysis could be performed that can provide valuable insights into the recruitment properties of the POI (e.g., contribution of multiple DNA binding domains, sensitivity towards different signaling events, etc.). Automated recruitment evaluation and cell tracking could be combined to create robust workflows [1,25].

Advantages and limitations of DNA pre-sensitization

Pre-sensitization of DNA prior to micro-irradiation is a commonly used tool for DNA repair protein recruitment[16,17]. Sensitizing DNA prior to micro-irradiation leaves it more susceptible to DSBs. The two most common methods for DNA pre-sensitization are pre-treatment of cells with either Bromodeoxyuridine (BrdU) or Hoechst dye. For systems not capable of micro-irradiation at high laser powers, these methods may be necessary for inducing DNA lesions like DSBs. Additionally, in the absence of a transmitted light detector or a fluorescent signal highlighting the cell nucleus (for example, when studying the recruitment of untagged endogenous DNA repair proteins), Hoechst acts as both a pre-sensitizing tool and a fluorescent nuclear stain. However, DNA pre-sensitization can introduce significant complications. BrdU (used at a final concentration of 10 μM) must be added to cells 24 hours (or time equivalent to a full cell cycle in the cell line used) to properly incorporate into DNA and can cause cell cycle interference[26]. Hoechst 33342 (used at a final concentration of 1 μg/mL) is cytotoxic in the long run, which can introduce irregularities in experimentation, therefore, should only be applied 15-20 minutes before micro-irradiation (enough time must pass to saturate the nucleus with the dye, otherwise the recruitment data will not be consistent). The cells stained this way cannot be kept in culture for more than a few hours[27,28]. Make sure not to use Hoechst 33358, which is not as cell permeable as the Hoechst 33342 dye. Pre-sensitization can also introduce unnecessary variance among experiments and makes the experiment even more sensitive to differences in cell density (as this will affect the amount of incorporated dye / cell).

Advantages and limitations of confocal microscopy

Imaging speed of confocal microscopy can be limiting when compared to widefield microcopy. However, a confocal microscope equipped with a resonant scanner can tremendously improve imaging speed (at the cost of resolution) coming close to speeds of spinning-disk microscopy. Three features make the A1R HD25 confocal system an excellent choice for the protocol

presented here. First, the 25 mm FOV of the system makes it possible to image between 15-20 cells in a single scanned field (vs. 5-10 cells in regular setups), limiting the number of acquisitions necessary to get enough cells for statistical analysis. Second, the FRAP module and two scanheads make it possible to image and micro-irradiate the cells simultaneously, not just sequentially. Lastly, the flexibility of having both the resonant and galvano scanners provides the ability to easily switch between high-temporal resolution imaging with exceptional speed which minimizes quenching of fluorophores, and high-spatial resolution imaging that utilizes slower scanning speeds to produce images with a higher signal to noise ratio. While the used system allowed for the aforementioned flexibility, to resemble more widely available confocal microscope configurations, only the galvano scanner was used in the presented experiments (for both micro-irradiation and subsequent imaging).

Advantages and limitations of micro-irradiation

While micro-irradiation provides unrivaled spatial and temporal resolution, it is not without limitations. DNA damage by laser micro-irradiation is highly clustered to specific parts of the nucleus compared to naturally occurring damaging agents. Thus, chromatin response due to micro-irradiation may differ compared to homogeneously distributed damage. Additionally, micro-irradiation is time consuming and may only be conducted on a few dozen cells, while large population-based biochemical methods (chromatin fractionation, immunoprecipitation, ChIP) can provide increased robustness by studying thousands of cells at a time. Verifying observations made by micro-irradiation with traditional biochemical techniques is an effective strategy for reliable conclusions. Though simultaneous micro-irradiation of many cells in a certain FOV is possible, the imaging system will need more time to perform the task. Therefore, measuring the dynamics of proteins that recruit very rapidly to DNA lesions limits the number of possible ROIs for micro-irradiation used simultaneously. On the imaging system used for this protocol, the micro-irradiation of a single 1024 pixel long ROI takes 1032 ms using 1000 μs dwell time and 3088 ms using 3000 μs dwell time to complete. Using multiple lines of ROIs will significantly increase the time needed to finish micro-irradiation (e.g., 7 x 1024 pixel long ROI takes 14402 ms using 1000 μs dwell time and 21598 ms using 3000 μs dwell time). This time is lost from image acquisition and must be taken into consideration. When imaging rapid recruitment events, use the shortest ROI possible and only micro-irradiate one cell at a time.

Advantages and limitations over synchronization methods

For cell cycle specific studies, the existing methods involve either the synchronization of cells into specific cell cycle phases or using fluorescent reporters to identify the specific cell cycle phase of the cell. However, each of these methods provides their own challenges and limitations.

The FUCCI system[3] (relying on fluorescent protein tagged truncated forms of CDT1 and Geminin) is a particularly useful tool for cell cycle studies but has limitations when it comes to differentiating between S and G2 phases of the cell cycle. Geminin levels are already high from mid S phase and stay high until M phase, making these phases difficult to separate. Using the FUCCI system also means that two optical channels of the microscope cannot be used for imaging the POI.

Non-cancer cell lines could be synchronized into G0 by the removal of growth factors found in the serum (serum starvation) causing little or no DNA damage to the cells. However, most cancer cell lines will partially continue to progress through cell cycle even without adequate amounts of serum in their media. Additionally, cells partially begin to lose synchronization by late G1, early S phase. In addition to serum starvation, there are numerous chemical methods to achieve cell cycle synchronization. Hydroxyurea, aphidicolin, and thymidine blocks are methods of stopping DNA replication to synchronize cells into early S phase. While these methods are cheap and simple, they introduce replication stress which results in DNA damage. These DNA replication inhibitors have been shown to induce the phosphorylation of H2A.X, a well-known marker of DSBs[2,29]. The method of using tagged-PCNA as a marker for S-phase cells reduces potential for artefacts caused by chemical synchronization and can be applied to a wide range of cell lines compared to serum starvation.

Conclusion

DNA damage is a driving force for genetic diseases where mutagenic lesions can lead to the malignant transformation of cells. Targeting the DNA synthesis machinery is a fundamental therapeutic strategy in treatment of hyperproliferative diseases like cancer. In order to treat these diseases in a more targeted fashion, we need a better understanding of the proteins that repair DNA lesions. The protocol described here helps micro-irradiation based studies in S phase by minimizing the challenges presented by traditional synchronization methods to reduce possible artefacts and increase the reproducibility of the experiments.

DISCLOSURES:

The authors state that the publication of the presented work was sponsored by Nikon Corporation. The authors declare that no competing interests exist.

ACKNOWLEDGMENTS:

The authors thank M. Pagano for his continuous support as well as D. Simoneschi, A. Marzio and G. Tang for their critical review of the manuscript. B. Miwatani-Minter thanks R. Miwatani and B. Minter for their continued support. G. Rona thanks K. Ronane Jurasz and G. Rona for their continued support.

REFERENCES:

1 Aleksandrov, R. et al. Protein dynamics in complex DNA lesions. *Molecular Cell.* **69** (6), 1046-1061 e1045 (2018).

2 Darzynkiewicz, Z., Halicka, H. D., Zhao, H., Podhorecka, M. Cell synchronization by inhibitors of DNA replication induces replication stress and DNA damage response: Analysis by flow cytometry. *Methods in Molecular Biology.* **761**, 85-96 (2011).

3 Sakaue-Sawano, A. et al. Visualizing spatiotemporal dynamics of multicellular cell-cycle progression. *Cell.* **132** (3), 487-498 (2008).

4 Herce, H. D., Rajan, M., Lattig-Tunnemann, G., Fillies, M., Cardoso, M. C. A novel cell permeable DNA replication and repair marker. *Nucleus.* **5** (6), 590-600 (2014).

5 Keijzers, G. et al. Human exonuclease 1 (EXO1) regulatory functions in dna replication with putative roles in cancer. *International Journal of Molecular Sciences.* **20** (1), (2018).

6 Cheruiyot, A. et al. Poly(ADP-ribose)-binding promotes Exo1 damage recruitment and suppresses its nuclease activities. *DNA Repair (Amsterdam).* **35**, 106-115 (2015).
7 Zhang, F., Shi, J., Chen, S. H., Bian, C., Yu, X. The PIN domain of EXO1 recognizes poly(ADP-ribose) in DNA damage response. *Nucleic Acids Research.* **43** (22), 10782-10794 (2015).
8 Rona, G. et al. PARP1-dependent recruitment of the FBXL10-RNF68-RNF2 ubiquitin ligase to sites of DNA damage controls H2A.Z loading. *elife.* **7**, (2018).
9 Young, L. M. et al. TIMELESS forms a complex with PARP1 distinct from its complex with TIPIN and plays a role in the dna damage response. *Cell Reports.* **13** (3), 451-459 (2015).
10 Kong, X. et al. Laser microirradiation to study in vivo cellular responses to simple and complex dna damage. *Journal of Visualized Experiments.* (131), e56213 (2018).
11 Kong, X. et al. Condensin I recruitment to base damage-enriched DNA lesions is modulated by PARP1. *PLoS One.* **6** (8), e23548 (2011).
12 Lan, L. et al. Novel method for site-specific induction of oxidative DNA damage reveals differences in recruitment of repair proteins to heterochromatin and euchromatin. *Nucleic Acids Research.* **42** (4), 2330-2345 (2014).
13 Zerjatke, T. et al. Quantitative cell cycle analysis based on an endogenous all-in-one reporter for cell tracking and classification. *Cell Reports.* **19** (9), 1953-1966 (2017).
14 Ji, Y., Karbaschi, M., Cooke, M. S. Mycoplasma infection of cultured cells induces oxidative stress and attenuates cellular base excision repair activity. *Mutation Research.* **845**, 403054 (2019).
15 Sun, G. et al. Mycoplasma pneumoniae infection induces reactive oxygen species and DNA damage in A549 human lung carcinoma cells. *Infection and Immunity.* **76** (10), 4405-4413 (2008).
16 Gassman, N. R., Wilson, S. H. Micro-irradiation tools to visualize base excision repair and single-strand break repair. *DNA Repair (Amsterdam).* **31**, 52-63 (2015).
17 Muster, B., Rapp, A., Cardoso, M. C. Systematic analysis of DNA damage induction and DNA repair pathway activation by continuous wave visible light laser micro-irradiation. *AIMS Genetics.* **4** (1), 47-68 (2017).
18 Ikeda, S. et al. Purification and characterization of human NTH1, a homolog of Escherichia coli endonuclease III. Direct identification of Lys-212 as the active nucleophilic residue. *Journal of Biological Chemistry.* **273** (34), 21585-21593 (1998).
19 Rosenquist, T. A., Zharkov, D. O., Grollman, A. P. Cloning and characterization of a mammalian 8-oxoguanine DNA glycosylase. *Proceedings of the National Academy of Science U. S. A.* **94** (14), 7429-7434 (1997).
20 Reid, D. A. et al. Organization and dynamics of the nonhomologous end-joining machinery during DNA double-strand break repair. *Proceedings of the National Academy of Science U. S. A.* **112** (20), E2575-2584 (2015).
21 Taccioli, G. E. et al. Ku80: product of the XRCC5 gene and its role in DNA repair and V(D)J recombination. *Science.* **265** (5177), 1442-1445 (1994).
22 Marsin, S. et al. Role of XRCC1 in the coordination and stimulation of oxidative DNA damage repair initiated by the DNA glycosylase hOGG1. *Journal of Biological Chemistry.* **278** (45), 44068-44074 (2003).
23 Thompson, L. H., Brookman, K. W., Jones, N. J., Allen, S. A., Carrano, A. V. Molecular cloning of the human XRCC1 gene, which corrects defective DNA strand break repair and sister chromatid exchange. *Molecular and Cell Biology.* **10** (12), 6160-6171 (1990).

24 Scharer, O. D. Nucleotide excision repair in eukaryotes. *Cold Spring Harbor Perspective Biology.* **5** (10), a012609 (2013).
25 Oeck, S. et al. High-throughput evaluation of protein migration and localization after laser micro-irradiation. *Science Reports.* **9** (1), 3148 (2019).
26 Mistrik, M. et al. Cells and stripes: A novel quantitative photo-manipulation technique. *Science Reports.* **6**, 19567 (2016).
27 Durand, R. E., Olive, P. L. Cytotoxicity, mutagenicity and dna damage by hoechst 33342. *Journal of Histochemistry and Cytochemistry.* **30** (2), 111-116 (1982).
28 Tobey, R. A., Oishi, N., Crissman, H. A. Cell cycle synchronization: reversible induction of G2 synchrony in cultured rodent and human diploid fibroblasts. *Proceedings of the National Academy of Science U. S. A.* **87** (13), 5104-5108 (1990).
29 Podhorecka, M., Skladanowski, A., Bozko, P. H2AX phosphorylation: Its role in DNA damage response and cancer therapy. *Journal of Nucleic Acids.* **2010**, (2010).

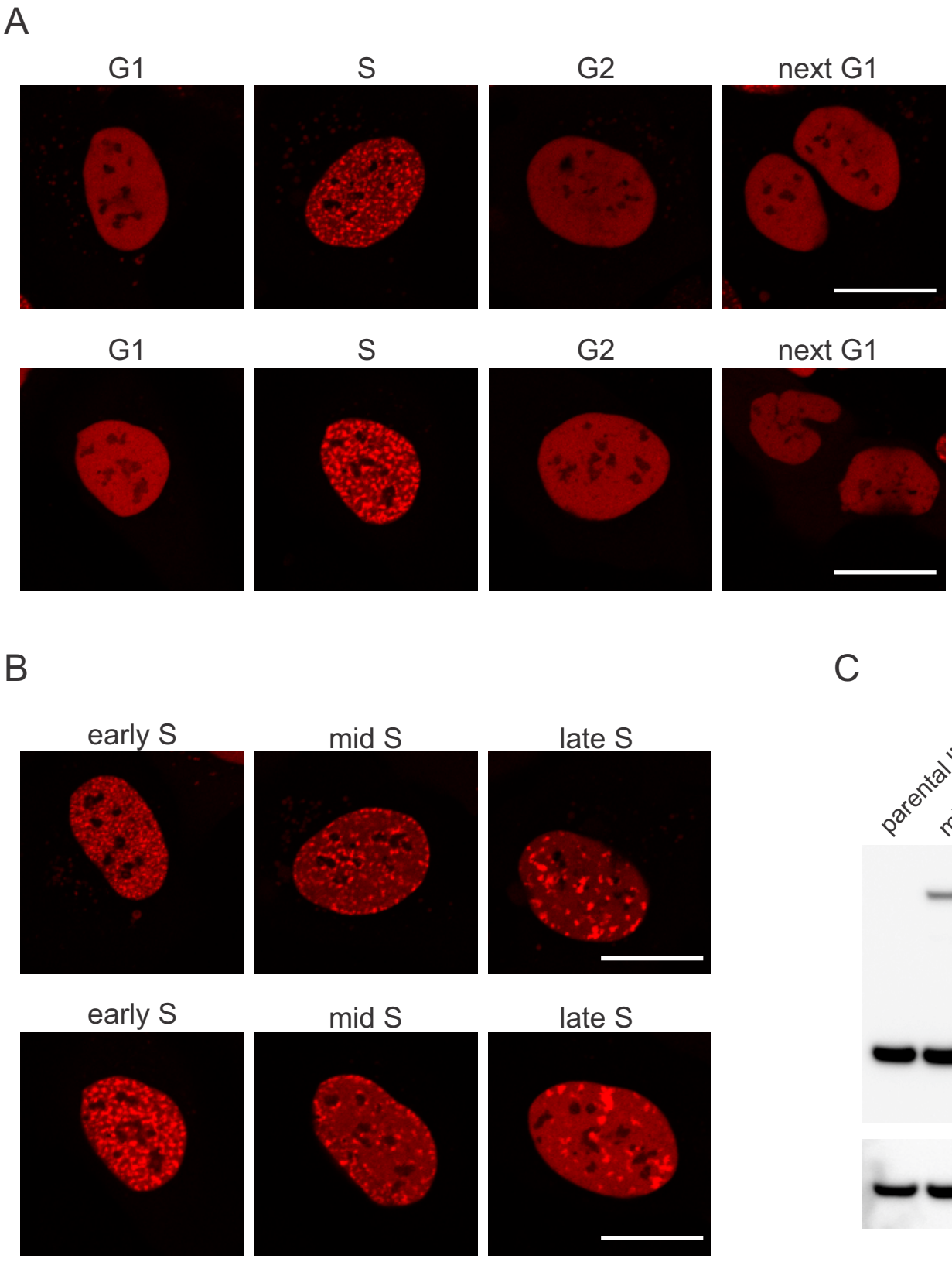

Figure 1, Miwatani-Minter *et al.*

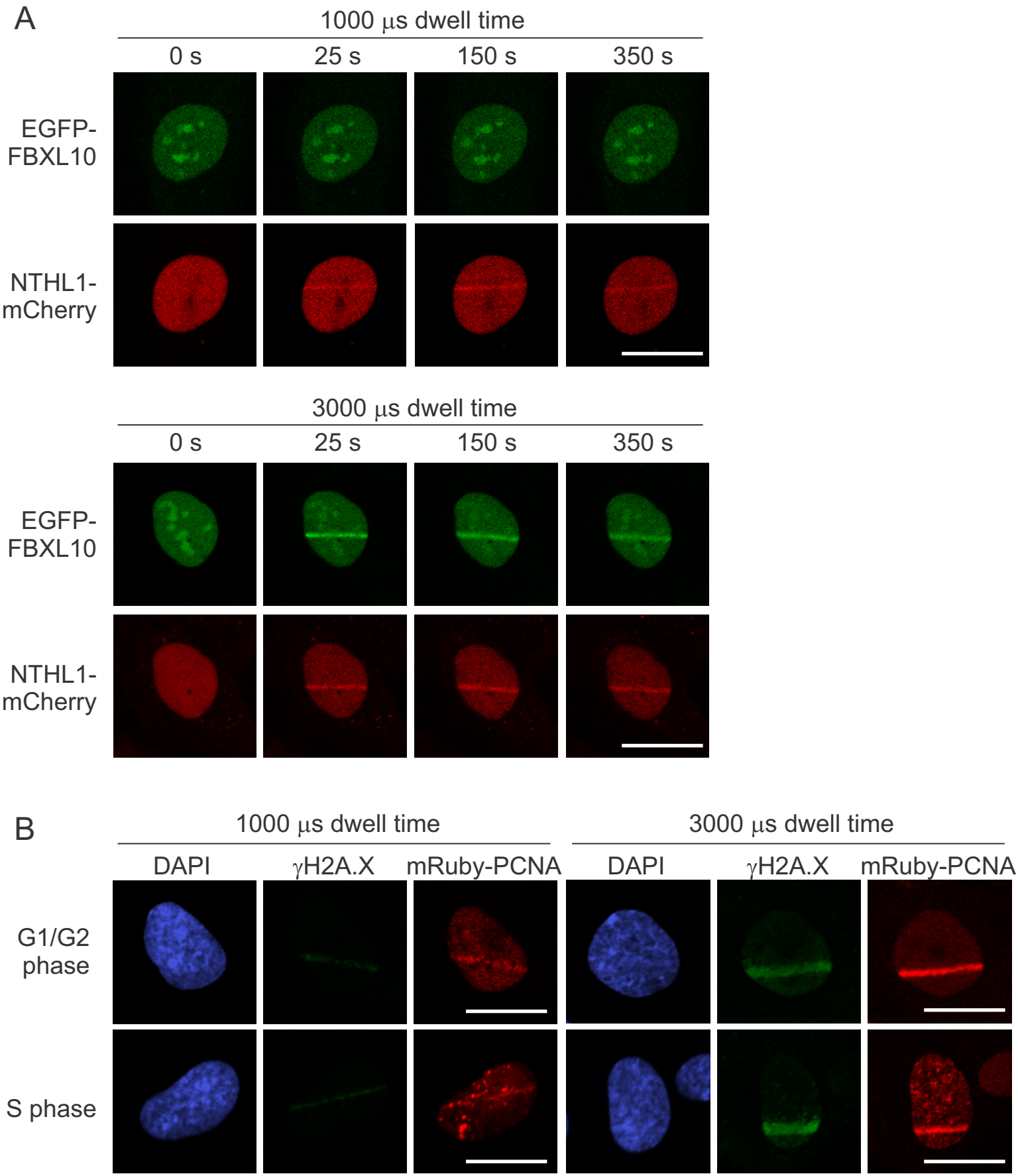

Figure 2, Miwatani-Minter *et al.*

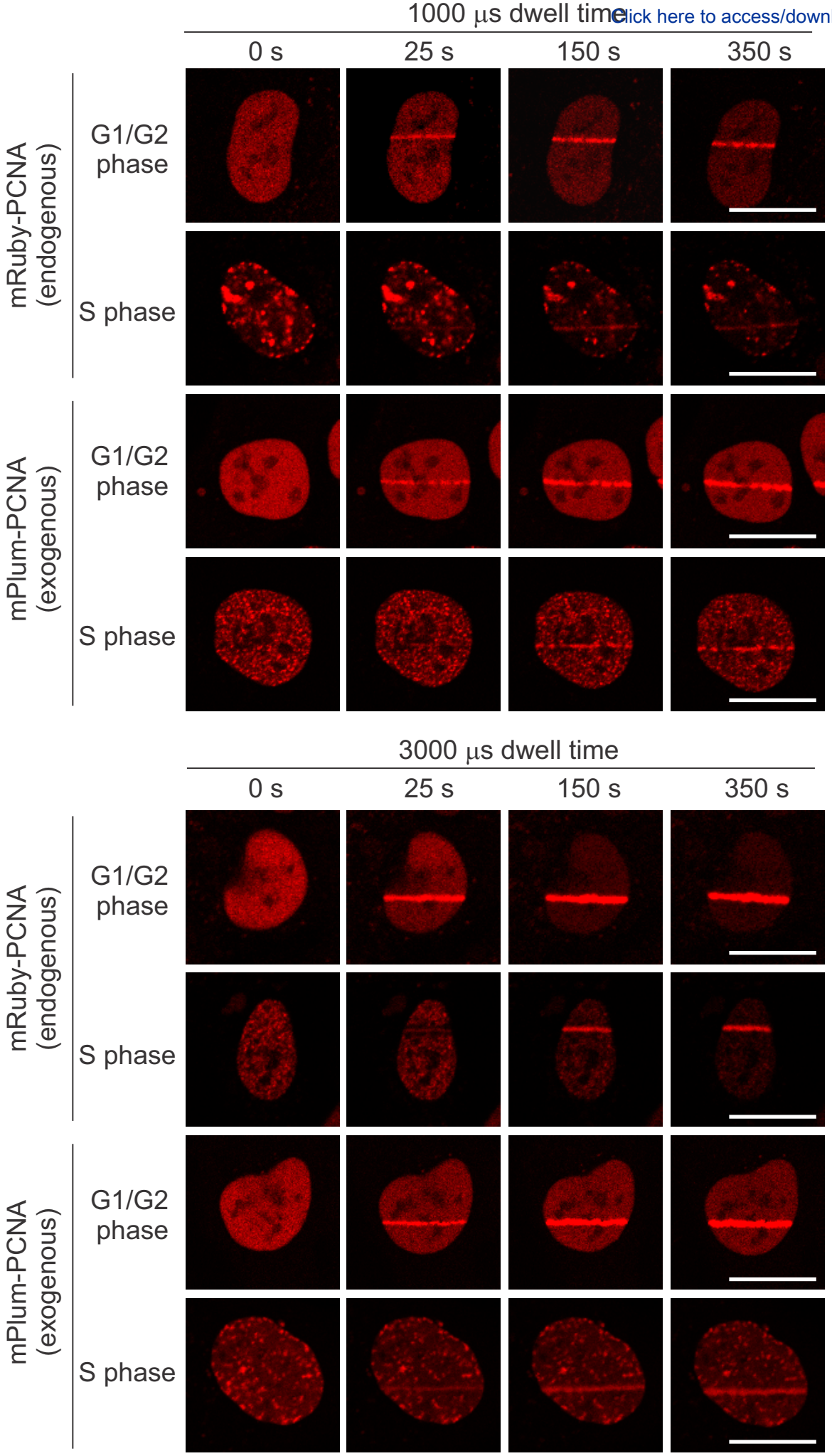

Figure 3, Miwatani-Minter *et al.*

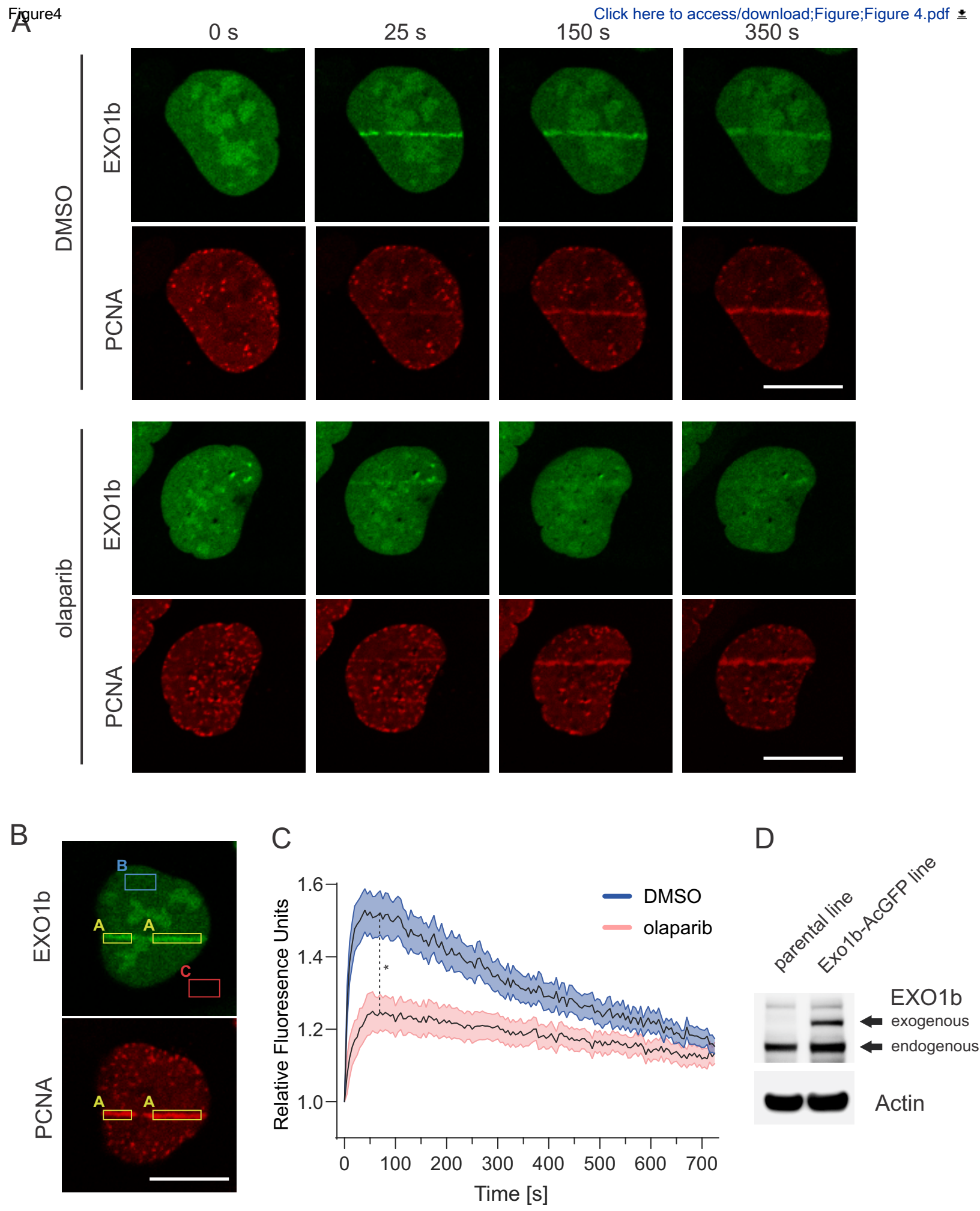

Figure 4, Miwatani-Minter *et al.*

Table of Materials

Click here to access/download;Table of Materials;Miwatani-Minter et al_Materials-edited.xls

Name of Material/ Equipment	Company	Catalog Number
Ammonium chloride	Sigma-Aldrich	A9434-500G
Anti-EXO1 Rabbit Polyclonal Antibody	Proteintech	16253-1-AP
Anti-phospho-Histone H2A.X (Ser139) Antibody, clone JBW301	Millipore	05-636
Bovine Serum Albumin	Sigma-Aldrich	3117332001
BrdU (5-Bromo-2'-deoxyuridine)	Merck	19-160
Citifluor™ Mountant Solution AFR3	Electron Microscopy Sciences	17973-10
DAPI	Sigma-Aldrich	D9542-1MG
DMEM Medium	Thermo Fisher Scientific	10569010
DMSO	Sigma-Aldrich	D2650-100ML
EGFP-FBXL10	Addgene	#126542
EXO1b-AcGFP (in pRetroQ)	custom cloning	na
Fetal Bovine Serum	Gibco	16140071
FluoroBrite DMEM	Thermo Fisher Scientific	A1896701
Goat anti-Mouse IgG (H+L) Highly Cross-Adsorbed Secondary Antibody, Alexa Fluor Plus 488	Thermo Fisher Scientific	A32723
HEK293T cells	ATCC	ATCC CRL-3216
HEPES	Sigma-Aldrich	H0887-100ML
Hoechst 33342	Thermo Fisher Scientific	H3570
Lipofectamine 3000	Thermo Fisher Scientific	L3000015
McCoy’s 5A (Modified) Medium	Life Technologies	16600-108
mCherry-PCNA	Addgene	#55117
mPlum-PCNA	Addgene	#55994
mPlum-PCNA (in pBABE)	custom cloning	na
Nikon A1R-HD25 Confocal Scanhead and Controller	Nikon	na
Nikon LUN4 laser unit	Nikon	na

Nikon LUN-F 50 mW 405 nm FRAP laser unit	Nikon	na
Nikon NIS Elements Confocal Controller Software	Nikon	na
Nikon Ti2-E Inverted Microscope	Nikon	na
Nikon Ti2-LAPP Modular Illumination System	Nikon	na
NTHL1-mCherry (in pRetroQ)	custom cloning	na
Nunc Lab-Tek II Chambered Coverglass (4 well)	Thermo Fisher Scientific	155382PK
Olaparib	Selleck Chemicals	S1060
Opti-MEM reduced serum media	Thermo Fisher Scientific	31985062
Paraformaldehyde aqueous solution (32%)	Thermo Fisher Scientific	50-980-494
pBABE (hygro)	Addgene	#1765
pBABE (neo)	Addgene	#1767
pBABE (puro)	Addgene	#1764
pBABE (zeo)	Addgene	#1766
PCNA Antibody (PC10)	Santa Cruz	sc-56
Penicillin-Streptomycin-Glutamine (100x)	Gibco	10378016
polybrene	Sigma-Aldrich	TR-1003
pRetroQ-AcGFP-C1	Takara	632506
pRetroQ-AcGFP-N1	Takara	632505
pRetroQ-mCherry-C1	Takara	632567
pRetroQ-mCherry-N1	Takara	632568
pUMVC	Addgene	#8449
Sodium-pyruvate	Thermo Fisher Scientific	11360070
Triton X-100 aqueous solution (10%)	Sigma-Aldrich	11332481001
Trypsin-EDTA Solution 10X	Sigma-Aldrich	59418C-100ML
U-2 OS Cells	ATCC	HTB-96
Universal Mycoplasma Detection Kit	ATCC	30-1012K
VSV-G	Addgene	#8454

Comments/Description
For quenching formaldehyde
primary antibody
primary antibody
BSA for blocking
pre-sensitizing agent
antifade containing PBS solution for imaging
nucleic acid stain
Cell culture medium for HEK293T cells
Vehichle control and dissolution solvent
viral expression vector for EGFP-FBXL10
EXO1b cDNA was cloned in the NheI, BamHI sites of pRetroQ-AcGFP1-N1 vector.
Media supplement
Phenol red free medium for microscopy
secondary antibody
Cell line for viral packaging
Buffering agent to supplement live cell imaging medium
pre-sensitizing agent
Transfection reagent
Cell culture medium for U-2 OS cells
non-viral PCNA construct suitable for cell cycle marker
non-viral PCNA construct suitable for cell cycle marker
mPlum-PCNA cDNA was cloned from Addgene #55994 in the BamHI, SalI sites of pBABE (puro)
confocal imaging system
excitation system

FRAP laser unit
Confocal controlling software
inverted epifluorescent microscope base
illumination system
NTHL1 cDNA was cloned in the NheI, SalI sites of pRetroQ-mCherry-N1 vector.

Live cell microscopy cell culture chamber
PARP inhibitor

Dilution medium for transient transfection

Fixative
retroviral expression vector (for low expression levels)
retroviral expression vector (for low expression levels)
retroviral expression vector (for low expression levels)
retroviral expression vector (for low expression levels)
primary antibody
Media supplement
Increase viral infection efficiency
retroviral expression vector
retroviral expression vector
retroviral expression vector
retroviral expression vector
Viral packaging vector

Supplement for live cell imaging medium
Dilute in PBS for cell permeabilization buffer
Dilute in PBS to split cells
Optimal cell line for microscopy experiments
PCR based Mycoplasma detection kit
Viral protein envelope vector

NYU School of Medicine

Dear Dr. Vineeta Bajaj and Dr. Lyndsay Troyer,

Enclosed is the revised version of our manuscript (tracking number # JoVE62466) in which we have addressed all the points raised by the reviewers, as described below:

Editorial comments (*italicized in blue*)

1. Please take this opportunity to thoroughly proofread the manuscript to ensure that there are no spelling or grammar issues.
Done.

2. Do not underline any part of the text.
All underlined text has been removed.

3. Use "mL" instead of "ml" (line 136). Add a single space between the quantity and its unit. E.g. "450 nm" instead of "405nm" (line 179).
The highlighted mistakes have been corrected.

4. Include a single line space between successive protocol steps and then ensure that the highlight is no more than 3 pages including headings and spacings. Avoid the use of personal pronouns in the protocol. E.g. "we", "our" etc.
Personal pronouns have been removed from the manuscript.

5. In the JoVE Protocol format, "Notes" should be concise and used sparingly. They should only be used to provide extraneous details, optional steps, or recommendations that are not critical to a step. Any text that provides details about how to perform a particular step should be written in imperative tense (as if telling someone how to do the technique), and either be included in the step itself or added as a sub-step. Do not include "notes" as protocol steps. E.g. line 211. Consider moving some of the notes about the protocol to the discussion section.
Notes sections have been trimmed down and in some sections of the protocol, notes have been moved to the discussion.

6. JoVE cannot publish manuscripts containing commercial language. This includes trademark symbols (™), registered symbols (®), and company names before an instrument or reagent. Please remove all commercial language from your manuscript and use generic terms instead. All commercial products should be sufficiently referenced in the Table of Materials. E.g. Nikon, Nunc, etc.
Commercial language has been removed from the text.

7. Figure 2, 3: Use "s" instead of "sec" in the labels.
"Sec" has been changed to "s" in all relevant figures.

8. Please ensure that the references appear as the following: [Lastname, F.I., LastName, F.I., LastName, F.I. Article Title. Source. Volume (Issue), FirstPage – LastPage (YEAR).] For more than 6 authors, list only the first author then et al. Do not abbreviate journal names. Do not use "&/and" in the authors list of the references. Please include volume and issue numbers for all references.
Endnote style from JoVe was used to format the Reference section.

9. Please ensure that all materials used are included in the table of materials.
Table of Materials has been updated to include all materials used.

NYU School of Medicine

Reviewer #1 (*italicized in blue*)

Major Comments:

** Chapter 1. (Cultivation of U-2 OS cell) is written too vague. Authors should give either number of the cells per ml or cm2. Otherwise, the cultivation lacks the consistency, 90% of confluency and split cells 1:10th is instruction based only on subjective feeling. It could be misleading for students as well as for early-stage researchers who start with cell cultivation methods.*

Protocol for the cultivation of U-2 OS cells have been updated in the text following the reviewers' recommendations. Exact cell numbers for during splitting are now included in the protocol.

** Section 3.3. How did authors established the final concentration of olaparib (1μM and one hour prior to irradiation experiments)? It seems to be a very short time to induce any changes in the accumulation of PCNA or EXO1b. Figure 3A is not convincing either, because there are different fluorescence intensities in red channels (DMSO vs olaparib). Lower accumulation of PCNA after 1 h olaparib treatment (25 sec after irradiation) could be only a matter of higher background in the individual cell. Also, there is no change in accumulation in EXO1b protein after olaparib treatment compared to DMSO control.*

We have now included further references in the text for the routine use of PARP inhibitors at the indicated concentrations and time, prior to micro-irradiation (PMID: 29985131, PMID: 26456830, 29547717). Olaparib treatment does not cause changes in the total protein levels of PCNA or EXO1b. However, it has been reported to affect the extent of EXO1b recruitment and delay PCNA recruitment, in line with our results shown in Figure 4 (PMID: 26519824, PMID: 26400172, PMID: 29547717). Any minor differences in the total fluorescence intensity of each cell (as seen on the representative images), comes from the fact that we used a heterogenous population of cells after viral infection. Depending on the amount of viral integration events in each individual cell, cells can express different levels of the POI. Importantly, our evaluation method (PMID: 29985131, PMID: 26456830) normalizes the recruitment intensities to the unaffected areas of the nucleus, therefore the experiments are internally normalized to the overall expression level of the POI in each cell. Establishing clonal cell lines is possible, but we would not recommend them for routine use due to increased possibility of artefacts (cherry picking clones from a heterogenous genetic background), therefore we omitted that approach from our protocol. We have changed the representative images on Figure 4A to be more in line with the graph shown in Figure 4C.

** Chapter 4. Authors stated that they used Nikon LUN-F 50 mW 405nm FRAP laser. What was the final dose (laser output behind objective) that was used to induced DDR?*

In terms of the laser power, the output behind objective depends on many factors including the optical fiber, the optical properties of all the lenses and mirrors in the light path, as well as the percent power output set in the software. Usually, the power controls in NIS elements are adjusted to be linear but it isn't always perfect. The laser power reaching the cells also depends on the immersion oil and the cell culture dish used. Because there are so many variables, we do not provide estimated power output behind the objective. Recommending a power meter in the protocol to measure it directly is simply not a realistic approach for most of the laboratories. Therefore, we propose in the protocol to use well characterized repair proteins to monitor the types of lesions generated (see Figure 2 and Discussion).

** Section 4.2.2. Authors stated that they selected FOV (field of view). Did authors select the same size of FOV per each irradiation experiment or it was different? Will the different size of FOV influence the intensity of the laser/ dose and the accumulation of POI to DNA lesions?*

The same size FOV (1024x1024 pixels) and zoom (1x) was used for each irradiation experiment to ensure the same pixel size (which was 0.29 μm/pixel) throughout our experiments. Because laser dwell time is on a per pixel basis, as long as the pixel size remains the same, the relationship between the dwell time and power density will not change. If the pixels size changes due to changes in the FOV and zoom settings the pixels would represent a different size area on the sample, making comparisons not possible. We have incorporated this information into the text (section 5.1.1).

** Chapter 5. How did the authors verify the appropriate laser power setting? Did the irradiated cells proceed to the mitosis? Please, provide relevant images.*

Appropriate laser settings were determined based on the ability to induce the recruitment of PCNA, FBXL10, NTHL1 and EXO1b with the minimum necessary laser power. Cells were not followed into mitosis. Whether cells enter mitosis or eventually progress through the next G1 phase depends on several factors. Even a very limited number of DSBs can delay or stop cell cycle progression until the damage is resolved otherwise cells go through to apoptosis (PMID: 30184135). Cell fate after DNA damage is ultimately dictated by p53 levels (PMID: 27062928, PMID: 30254262, PMID: 28317845) therefore, the p53 background of the cell lines used, will dramatically affect whether they will enter mitosis or not. U-2 OS and RPE cells used in our protocol have a functional p53 response therefore being more sensitive towards the recovery from laser induced DSBs. HeLa cells, lacking functional p53, would show a more robust entry into mitosis. The focus of our protocol was to visualize repair processes in S phase, therefore studying mitotic entry was out of our scope.

** Either stable or transient transfection of proteins may bypass regular expression, did authors verify their observations by immunofluorescent labelling of endogenous accumulation PCNA and other POI after irradiation? Please, provide relevant comparative images.*

Recruitment of tagged exogenous PCNA has been well established in the literature (PMID: 25484186) therefore we did not perform immunofluorescent staining against endogenous PCNA. One of the fundamental limitations of that approach is the lack of temporal dynamics since one uses fixed cells. Therefore, to demonstrate the recruitment of endogenous PCNA in our experimental setup, we have used human retinal pigment epithelial cells (hTERT RPE-1) in which the fluorescent protein mRuby was engineered in frame with the first exon into one allele of the PCNA locus by recombinant adeno-associated virus-mediated (rAAV) homologous recombination in (the cell line was a kind gift of Jörg Mansfeld) (PMID: 28564611). Cell cycle based localization pattern was identical to our findings using exogenous PCNA. Results are shown on the new Figure 3 and updates have been made in the text accordingly.

Minor Comments:

** Section 2.1. In the manuscripts, there is no information regarding cultivation conditions (media etc.) of HEK293T cells*

Cultivation of HEK293T cells is now incorporated in the protocol. Please see section 2.1.1.

** Row 161: …plate 8.0x104 cells… per what volume?*

$8.0x10^4$ refers to the total number of cells plated into the four-well chamber. Any volume between 0.5 mL and 1 mL is sufficient for culturing in a 4 well chamber. We have updated the text to be less confusing in section 3.1.

Table of Material:

** Unify HEK293T cell or 293T cells*

293T has been changed to HEK293T in the table of materials.

** No standard DMEM Medium is mention in the Protocol*
Cultivation of HEK293T has been added to the protocol which now mentions standard DMEM Medium.

** No pre-sensitizes were used in Protocol. Why are Hoechst 33342 and BrdU mentioned in Table of Material?*
Hoechst 33342 and BrdU were discussed extensively in the Discussion and were included in the Table of Materials for the readers convenience if relevant to their experimentation.

** No Nunc™ Lab-Tek™ II Chambered Coverglass (8 well) is used in the Protocol*
Lab-Tek™ II Chambered Coverglass (8 well) has been removed from the Table of Materials.

** No Universal Mycoplasma Detection Kit is mentioned or used in the Protocol*
Use of the Universal Mycoplasma Detection Kit has been now placed into the protocol.

Reviewer #2 (*italicized in blue*)

Major Comments:
1) The manuscript contains many paragraphs unaccompanied by supporting citations. The introduction is currently too vague and lacks information about existing approaches to quantify protein recruitment to sites of DNA damage1. PCNA is a well-studied S-phase marker. It is widely used to identify S-phase cells in live cell fluorescence microscopy and to distinguish between cell-cycle specific differences of DNA damage response (DDR) protein dynamics2-4. Novelty of the method is not a pre-requisite for a JOVE publication, but I think it is particularly important to enable the scientific community to easily compare method papers by providing citations and that the introduction should provide a more through overview of existing methodology (beyond the example mentioned here). Similar to the introduction, the discussion is lacking the citation of supporting literature and a discussion of the obtained results in the context of existing literature. Additionally, the limitations imposed by the choice of slow confocal microscopy and "relative fluorescence unit" image analysis on the interpretation of recruitment kinetics results should be discussed.
We thank the reviewer for these recommendations. We have incorporated new citations throughout the manuscript accordingly. We have also added a paragraph in the discussion about the limitations of confocal microscopy. (Note: Unfortunately, we did not receive the exact recommended references of Reviewer 2.)

2) To verify that the 405 nm laser induces double-strand DNA breaks (DSBs) the laser dwell time at 50 mW power was increased until the induced damage was sufficient to observe recruitment of EGFP-FBXL10 (subunit of the FRUCC complex), a PARP1-dependent ubiquitin ligase complex previously reported to recruit to DSBs. This is a very indirect method to assess DSB induction. Instead, the cells should be fixed after laser damage and immunofluorescence with an antibody against a marker of DSBs such as γH2AX5, 6.
We performed immunofluorescence staining against γH2A.X in the micro-irradiated cells, confirming the elevated levels of DSBs when using a higher laser setting (Figure 2B). DSB induced recruitment of EGFP-FBXL10 has also been studied in detail (PMID: 29985131). We have also included a section on immunofluorescence staining this into the protocol (section 5.3) to check for γH2A.X saining.

3) Quantifying the recruitment of DDR proteins to sites of laser damage by measuring the fluorescence intensity has a major caveat that is not addressed in this manuscript but potentially affects the quality of the results shown in Figure 3A. There are bright spots close to the damage

site in Figure 3A, olaparib treated cells. These bright spots can easily skew the measurement of fluorescence intensity. In this respect the section about recruitment kinetics analysis is too vague and overall does not provide enough information to perform a reproducible quantification. For example, there is no mention of how big the analyzed regions "A", "B" and "C" should be and how to determine a suitable region "A" and "B" within the nucleus without skewing the quantification (e.g how to correct for bright foci or nucleoli within the region). This is essential for a manuscript that focuses on cells in S-phase as replication foci can provide a major source of artefacts in the quantification. The authors should further specify details regarding correcting for or preventing artefacts due to movements of the cells relative to the selected region across different timepoints. The authors should explain how ImageJ is used to perform these intensity measurements in a reproducible and automated manner and how the measurements across regions, timepoints and cells are collected and compiled to produce Figure 3B.

We have updated Section 6 of the protocol to contain more details on image analysis and important guidelines on the analyzed regions and possible artefacts (PMID: 29985131). We have also included a new representative image (Figure 4B) to aid evaluation in Section 6.

4) It would be useful for the authors to provide equations or mathematical models to extract information about the recruitment kinetics from the curves in Figure 3B. This section should be the main focus of this manuscript because the word "kinetics" implies that, at the very least, the authors will provide methods to calculate either the half time or the time when maximum recruitment is reached, and the time the intensity reaches a plateau. There are examples in the literature how to distinguish if two proteins have distinct kinetics, or merely different recruitment intensities with comparable kinetics7. I would also suggest that the authors compare the recruitment kinetics of Exo1b in S-phase cells vs G1 cells to support the statements in line 87/88 of the introduction. Furthermore, the authors say that Exo1b recruitment kinetics is changed in response to olaparib treatment. Based on the curves in Figure 3B, Exo1b reaches its maximum at around 60 seconds in both cases. According to the plots, the recruitment intensity is decreased in olaparib treated cells but based on the sample images in Figure 3A the recruitment intensity looks comparable between DMSO treatment and olaparib treatment at all three depicted timepoints.

We did not compare the recruitment profile of EXO1b in G1 vs. S-phase cells as our protocol only focuses on S phase (as part of the *Current methods to analyze DNA damage in S-phase in eukaryotic cells* JoVe methods collection). PCNA has a homogenous localization pattern in both G1 and G2 phases of the cell cycle (Figure 1) requiring additional synchronization steps to be able to evaluate just G1-phase cells. We agree with the reviewer that detailed kinetic analysis can provide valuable insights into the recruitment properties of the POI. However, in order to apply mathematical models, detailed characteristics of the recruitment has to be known (*e.g.*: contribution of multiple DNA binding domains, sensitivity towards different signaling events, *etc*.). The observed recruitment kinetics is the combined output of several factors which needs to be deconvolved into individual mechanistic contributors for proper mathematical modelling. We believe this in-depth analysis is out of the scope of this protocol and therefore we show recruitment profiles by connecting the RFU values over time, as also shown in the literature for EXO1b (PMID: 23939618, PMID: 26519824, PMID: 26884156, PMID: 26400172, PMID: 20019063). We have also corrected the text to reflect only the differences observed in the maximal extent of EXO1b accumulation (DMSO vs. olaparib), which is in agreement with the above cited literature. We removed “kinetics” from the title and the text and added additional references for optional kinetic analysis in the discussion.

5) Exo1b signal in Figure 3A is stronger in nucleoli. However, in previous literature the signal in the nucleus and the nucleoli is indistinguishable8, 9. In the cited papers Exo1b was tagged N-terminally and in this manuscript C-terminally. Could this explain the changed localization? In this

manuscript the maximum recruitment is reached after 1 minute whereas previously Exo1b was reported to reach a maximum up to 5 minutes after damage before starting to dissociate from damage sites8, 9. Could you clarify if this is due to different damaging conditions or if C-terminal tagging impairs the function and DNA damage recruitment of Exo1b? In Discussion line 376 you mention tagging can impair protein function so it would be good to check and compare the function, localization and recruitment of N- and C-terminally tagged Exo1b.

As mentioned by the reviewer the exact recruitment profile might rely on several factors, like the exact laser damage used (*e.g.:* 365 nm vs. 405 nm) or whether EXO1b is tagged either on the N or C-terminal in the studies. The PIN domain of EXO1b is on the N-terminal while the PIP motif is on the C-terminal, with both structural elements contributing to the recruitment of EXO1b. Both C-terminally: PMID: 29551515, PMID: 30622624, PMID: 26884156 as well as N-terminally: PMID: 26400172, PMID: 26519824, PMID: 20019063, PMID: 23939618 tagged EXO1b is used routinely in the literature. Localization pattern varies among these papers. In the above cited manuscripts, there are examples where EXO1b is excluded from the nucleoli, is evenly distributed in the nucleus or partially accumulates in the nucleoli (PMID: 26884156 as) we have seen it too. The localization pattern may rely on the expression levels of EXO1b, and the type of cell lines used in the different studies. Unfortunately, the exact EXO1 isoform used in the papers is not always specified. EXO1 has three isoforms, slightly differing from each other. We are using EXO1b, the longest isoform (PMID: 20019063, PMID: 29551515). It is also important to note that we were aiming to detect differences w/wo a specific treatment (in our case olaparib).

6) The authors mention in line 322-323 the importance of comparing the overexpression levels of the protein of interest to the endogenous levels. It would thus be useful to compare Exo1b overexpression and endogenous levels in U2OS cells.

We have now compared the expression levels of endogenous and exogenous EXO1b shown in Figure 4D. The expression level of EXO1b-AcGFP is similar to endogenous EXO1b.

7) In the methods the authors should mention the filters used in the microscopy setup. Especially as the authors state in line 255 that simultaneous imaging of Exo1b and PCNA was done, the authors should show a control sample to confirm no fluorescence bleed-through and cross-excitation is skewing the recruitment quantification. This will help readers to select filter sets and set up control experiments to avoid such artefacts.

We have now included in Section 4 the exact filters and lasers lines used for imaging, making a note on the importance of checking fluorescence bleed-through. We have also included here (see below) a panel showing that we did not have any fluorescence bleed-through with our imaging settings. Our protocol did not aim to cover basic confocal microscopy. We believe a laboratory routinely using fluorescent microscopy will have these appropriate controls already established before implementing our protocol.

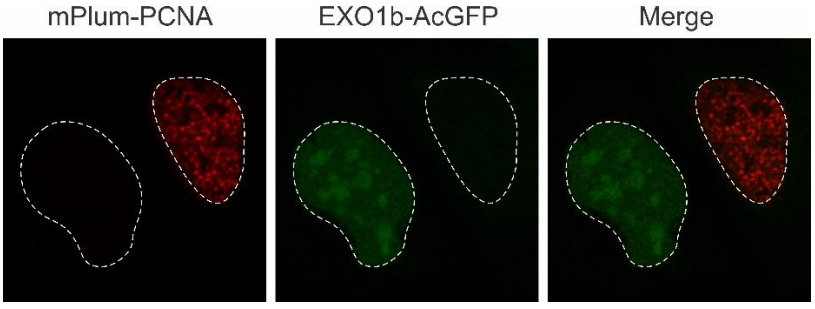

Since infection is not 100% efficient and we did not sort for double positive cells, we used the single-colored cells (either just mPlum-PCNA or EXO1b-AcGFP positive) to show the lack of bleed-through when using simultaneous excitation during our imaging.

8) Paragraph 4.2.5 is unclear. The authors should provide specific information about how long the microirradiation takes and how much time is lost before the software starts recording data for

the recruitment curve. In order to quantitively assess protein recruitment kinetics, the first few seconds after laser damage are essential and inconsistent start of acquisition after damage can severely skew the results. Line 219 is unclear. What does 0.5-2 µm thickness mean and how is this measured?

The Limitations of micro-irradiation section of the Discussion has been updated with the exact time needed to micro-irradiate cells using our protocol and imaging system. To avoid any confusion, we removed the 0.5-2 µm thickness note from the protocol that was referring to the thickness of a typical EXO1b recruitment track.

9) 5.1.1, line 234 and 5.2.1, line 251: the scanning speed has to be provided in a more useful unit like µs/pixel. The image size and zoom has to be amended by providing the resulting pixel size (µm per pixel) of the images. Otherwise fixing the pixel dwell time of the 405 nm FRAP laser may lead to variable results. 5.1.3, line 244, please clarify if 1000-3000 µs is the dwell time per pixel or the dwell time across the whole damage line. The exact length in pixels of the line along which the 405 nm laser damage was applied has to be provided.

Section 5.1.1 and 5.2.1 has been updated to reflect the scanning speed in µs/pixel. We have also included the pixel size that results from the image size and the zoom used in the protocol. We have updated the text in section 5.1.3 to clarify that the given laser dwell time is on a per pixel basis, not across the whole damage line (ROI). We have also included information on the exact length of the ROI used for micro-irradiation in pixels (section 4.3.5).

10) In 5.1.3, line 244 the resulting FRAP 405 nm laser power at the sample should be measured and provided as a reference to replicate the described experiments. Identical 50 mW lasers will produce different effective damage depending on the amount of light lost in the optical path.

In terms of the laser power, the output behind objective depends on many factors including the optical fiber, the optical properties of all the lenses and mirrors in the light path, as well as the percent power output set in the software. Usually, the power controls in NIS elements are adjusted to be linear but it isn't always perfect. The laser power reaching the cells also depends on the immersion oil and the cell culture dish used. Because there are so many variables, we do not provide estimated power output behind the objective. Recommending a power meter in the protocol to measure it directly is simply not a realistic approach for most of the laboratories. Therefore, we propose in the protocol to use well characterized repair proteins to monitor the types of lesions generated (see Figure 2 and Discussion).

11) In 5.2.2 the exact imaging conditions (type of excitation lasers and excitation power) used for the results presented in this manuscript should be provided.

Exact imaging conditions are now included in section 5.2.2.

12) Why was EGFP used for one experiment (EGFP-FBXL10) and AcGFP in the remaining experiments? Does AcGFP dimerize like GFP? Using a dimeric form of GFP would contradict the discussion line 376-378. Please clarify this.

We have used the EGFP-FBXL10 (in a pBABE.puro backbone) construct because it is conveniently deposited at Addgene (Plasmid #126542) so everyone can easily obtain it. The recruitment properties of EGFP-FBXL10 have been extensively characterized, making it an optimal choice for DSB detection (PMID: 29985131). To achieve comparable expression levels to endogenous EXO1b we needed a retroviral expression vector with a stronger promoter. For this purpose, we chose the pRetroQ vectors sold by Takara. Takara, the manufacturer selling AcGFP based plasmids states the following on their website: "AcGFP1 (*Aequorea coerulescens* GFP) is a monomeric green fluorescent protein with spectral properties similar to those of EGFP. Although AcGFP1 and EGFP sequences have 94% homology at the amino acid level and equivalent brightness, AcGFP1 is a superior alternative for fusion applications because it is a

monomer." In our opinion both EGFP and AcGFP can be used successfully in our protocols. We have updated the text to include more information on possible monomeric fluorescent proteins that could be used.

13) A previous publication showed no recruitment of NTHL1 to a 405 nm 50 mW laser10. Please comment on this discrepancy. This is particularly important because this experiment is used as an indirect indication for the presence of oxidative damage. In line with my major comment 2): Using the recruitment, or lack of recruitment of a protein to a laser damage site should not be used as the only indicator for the presence or absence of DNA damage, especially if the results show inconsistent recruitment across different publications.
We think the reviewer was referring to the following publication PMID: 24293652. (Note: Unfortunately, we did not receive the exact recommended references of Reviewer 2.) While the paper does not show recruitment of GFP-NTHL1 with using 50 mW laser power (405 nm), it does show recruitment by using 500 mW laser power (405 nm) or by the excitation of KillerRed (generating oxidative DNA damage). The authors indicate the amount of laser power used at each scan but did not define the exact FRAP area in pixels, therefore it is uncertain how much energy was actually delivered into a pixel: "405-nm laser light for 10 scans with a rate of 5 mW/scan (total 50 mW)." Additionally, the authors used transient transfection, that can result in high protein levels when comparing it to endogenous levels, therefore requiring more lesions to see signal accumulation at the damage site due of the high signal intensity in the surrounding nucleoplasm. GFP-NTHL1 was also shown to recruit to laser stripes induced with a 780 nm NIR laser line using adequate power to induce base damage (PMID: 29443023, PMID: 21858164). In summary we believe our results are in line with the literature.

Minor Comments:
1) The NTHL1-mCherry construct is missing from the materials list and a description or reference is missing of how U2OS cells for the experiments in Figure 2 were created.
We have updated the text to include information on how the NTHL1-mCherry construct and the stable U2OS cell line was generated sec 5.1.3. Details of the plasmids used can be found in the Table of Materials.

2) Line 43: mCherry PCNA mentioned in the abstract whereas the rest of the manuscript refers to mPlum PCNA. In the list of Materials mCherry PCNA is again mentioned but as far as I understood it has not been used.
The reviewer is correct and mCherry-PCNA has been corrected to mPlum-PCNA in the abstract.

3) Line 203: Sentence grammatically wrong
We have corrected the sentence.

4) Title is misleading and I suggest the following alternative: "Laser micro-irradiation to study protein recruitment to sites of DNA damage in S-phase"
We agree with the reviewer and we removed kinetics from our title as recommended.

5) The authors mention the importance of mycoplasma contamination in the discussion (lines 318-321) but it is unclear if and how the U2OS cells used in this experiment were tested for mycoplasma
Use of the Universal Mycoplasma Detection Kit has been now placed into the protocol.

Reviewer #3 (*italicized in blue*)

Minor Comments:

NYU School of Medicine

A discussion of the statistical methods that are appropriate to use when comparing recruitment kinetics across different conditions should be added. A preferred statistical test should also be used to demonstrate the significance of the difference in exo1b kinetics in DMSO- vs olaparib-treated cells the data presented in figure 3b.

We thank the reviewer for the suggestion and have added references to statistical methods and approaches on detailed kinetic analysis of the recruitment data in the discussion. We have also included the results of a two-tailed Mann-Whitney test to compare the maximum extent of EXO1b accumulation at 1 minutes between the DMSO and olaparib treated cells (Figure 4C).

Typos and syntax:

Line 30. Undermining the structures and functions of proteins and…
Line 76. lesions and is recruited to locally
Line 185. System be thermally
Line 198. In S-phase, PCNA forms…
Line 285. Homogeneous
Line 302 are recruited demonstrating
Line 308-309 is denoted by a > 1 relative….
Line 382 homogeneously
Line 445. Figure 3. PARP1/2-dependent (olaparib inhibits both enzymes)

The following suggestions have been implemented into the text.

We appreciate the constructive suggestions made by all reviewers, and we believe that the resulting additions and changes have improved the clarity and message of our study. If you have any further questions, please feel free to contact me. I look forward to hearing from you.

Sincerely,

Gergely Rona, PhD
Postdoctoral Fellow | The Pagano Lab
Dept. of Biochemistry & Molecular Pharmacology
NYU School of Medicine | Howard Hughes Medical Institute
450 E 29th St., Alexandria Center for Life Sciences, Room 843
New York, NY 10016

02/24/2021